

# 초청 강연 IV

X-ray PIV Measurements of Velocity Field of Blood Flows

- 좌장 | 삼성서울병원 김동익

- 포항공대 이상준

# X-ray PIV Measurements of Velocity Field of Blood Flows

Sang Joon Lee\* and Guk Bae Kim

Department of Mechanical Engineering, Pohang University of Science and Technology

## Abstract

The x-ray PIV method was improved for measuring quantitative velocity fields of real blood flows using a coherent synchrotron x-ray source. Without using any contrast media or seeding particles, this method can visualize flow pattern of blood by enhancing the phase-contrast and interference characteristics of blood cells based on a synchrotron x-ray imaging mechanism. The enhanced x-ray images were achieved by optimizing the sample-to-scintillator distance, the sample thickness, and hematocrit. The quantitative velocity fields of blood flows inside opaque tubes were obtained by applying a 2-frame PIV algorithm to the x-ray images of the blood flows. The measured velocity field data show typical features of blood flows such as the yield stress effect. The non-Newtonian flow characteristics of blood flows were analyzed using the x-ray PIV method and the experimental results were compared with hemodynamic models.

Keywords: x-ray PIV, flow pattern of blood, blood flow, phase-contrast

## Introduction:

Most of flow visualization techniques using visible light can be employed only for transparent fluids. They are unsuitable to visualize opaque fluids such as human blood, which is filled with RBCs (red blood cells) of about 37~45 % of the whole blood. For the case of blood flow inside a transparent microchannel, we can visualize a blood flow of shallow depth (*several tens* of microns) by tracing RBCs or tracer particles seeded in the blood using a visible light.<sup>1</sup> However, when the thickness of blood sample exceeds several hundred microns, the blood becomes to be opaque for visible light, making difficult to visualize the blood flow with conventional optical methods. Unfortunately, most important hemodynamic phenomena related with circulatory vascular diseases occur in the blood vessels of several

millimeters or even larger in diameters. Therefore, most of conventional flow visualization methods can not be used for visualizing real blood flows directly and for investigating hemodynamic phenomena of real blood.

Conventional medical instruments for diagnosing vascular diseases, such as angiography or Doppler techniques, give information on blood vessel shape or point-wise blood flow speed with poor spatial resolution. They cannot provide detailed quantitative information on the flows inside blood vessels with micrometer-scale spatial resolution such as a PIV (particle image velocimetry) velocity field measurement.

Most vascular diseases occur in blood vessels with diameters on the order of several hundreds micrometers or even larger. In addition, flow properties such as wall shear stress inside blood vessels play a key role in the pathology of atherosclerosis, underlining the importance of obtaining quantitative flow information related to such flow phenomena.<sup>2</sup> As mentioned above, optical flow visualization methods are unsuitable for measuring blood flows in relatively thick blood vessels because of

---

San 31, Hyo-Ja Dong, Pohang, 790-784, KOREA

E-mail : sjlee@postech.ac.kr

---

the poor permeability of such blood and blood vessels. On the other hand, medical instruments can penetrate blood vessels, but gives data with low spatial and temporal resolutions. Therefore, a new advanced visualization technique is needed for extracting quantitative information on the hemodynamic characteristics of blood flows in arteries and veins with diameters on the order of several millimeters. Such a visualization technique should have a light source that can penetrate flows in thick vessels, micrometer-scale spatial resolution, and temporal resolution that is sufficient for monitoring fast blood flows. In addition, it must be biologically safe.

To resolve the limitations encountered in optical flow visualization methods and conventional clinical instruments, we developed an x-ray PIV technique<sup>3</sup> and found its feasibility of visualizing a blood flow.<sup>4</sup> We investigated systematically the optical characteristics of blood for a coherent synchrotron x-ray more systematically with varying several parameters such as distance between the sample and scintillator, sample thickness and hematocrit.<sup>4</sup> In addition, we analyzed the non-Newtonian flow characteristics of blood moving in a circular tube and compared the experimental results with hemodynamic models.

## Materials and methods:

### **Characteristics of blood on x-ray imaging method**

To visualize blood flow inside an opaque conduit and analyze the flow characteristics quantitatively, we combined an x-ray micro-imaging technique and a PIV velocity field measurement technique. The third generation synchrotron radiation source of PLS (Pohang Light Source, Pohang, Korea) was used in this study. The high coherence of this light source offers various approaches to radiology.<sup>5-8</sup> Several imaging techniques utilizing coherent light sources, such as holography and interferometry, have been studied. In addition, some

phase contrast imaging methods have been developed.<sup>9-11</sup>

Two problems, however, have to be solved for applying the x-ray PIV technique to x-ray images of blood flows. At first, velocity field information is commonly extracted from flow images by tracking tracer particles seeded into the flow. However, the adulteration of blood with artificial tracer particles may alter the biochemical and flow characteristics of the blood, and may cause biological damage on the blood. Therefore, for investigating real blood flows, we should extract velocity information from the blood flow itself without adding any tracer particles. Second, because the biological specimens composed of low-density elements are transparent to hard x-rays, the conventional absorption-contrast x-ray imaging method is ineffective.<sup>12</sup> In addition, because the optical properties of RBCs and plasma are so similar, it is not easy to discriminate blood cells clearly even using the phase-contrast x-ray imaging method.

To resolve these problems, we captured speckle patterns of blood flow illuminated with a coherent synchrotron x-ray. The coherent x-rays induce classic Fresnel edge diffraction in radiological images. This Fresnel edge diffraction pattern, which consists of alternating bright and dark speckles, is formed as a result of interference between two differently phase-shifted waves passing through a test object. The speckles in the captured x-ray images make it easy to discern the edges of specimens such as RBCs. In general, the speckle patterns become clearer as the sample-to-scintillator distance  $d$  is increased. In the present experiments, we obtained x-ray images of blood flow using the propagation-based phase-contrast method after optimizing the sample-to-scintillator distance  $d$ .

Figure 1 shows the x-ray images of RBCs monolayer at four different distances  $d$ . For obtaining the x-ray images of RBCs, we used an unmonochromatic beam at 7B2 beam

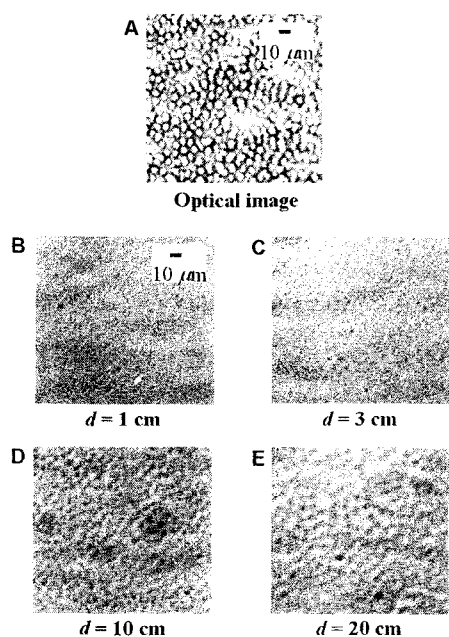


**Figure 1.** X-ray Images of RBC monolayer using the phase-contrast enhancement

line of PLS. The lateral resolution is less than  $0.7 \mu\text{m}$  and the size of source in the vertical and horizontal

directions are  $45 \mu\text{m}$  and  $120 \mu\text{m}$ , respectively. The beam characteristics and performance of this experimental beamline are described in Je *et al.*<sup>13</sup>

An optical image of the same RBC monolayer is included for comparison. The scale bar corresponds to  $10 \mu\text{m}$  and all images were captured under the same magnification. In the optical image (Fig. 1A), individual RBCs are clearly visualized. However, as shown in Figs. 1B and 1C, the RBCs cannot be discerned in the x-ray images obtained at small sample-to-scintillator distances ( $d = 1$  and  $3$  cm). When  $d$  is increased beyond  $3$  cm, RBC speckle patterns become clearer (Figs. 1D and 1E). Comparison of the size of RBCs appeared in the optical image and the speckle patterns in the x-ray images confirm that the speckle patterns originate directly from the RBCs. It is worthwhile to note that the phase-contrast enhancement method can visualize blood cells without magnification optics such as a zone-plate, a Kirkpatrick-Baez mirror, or a compound refractive lens.

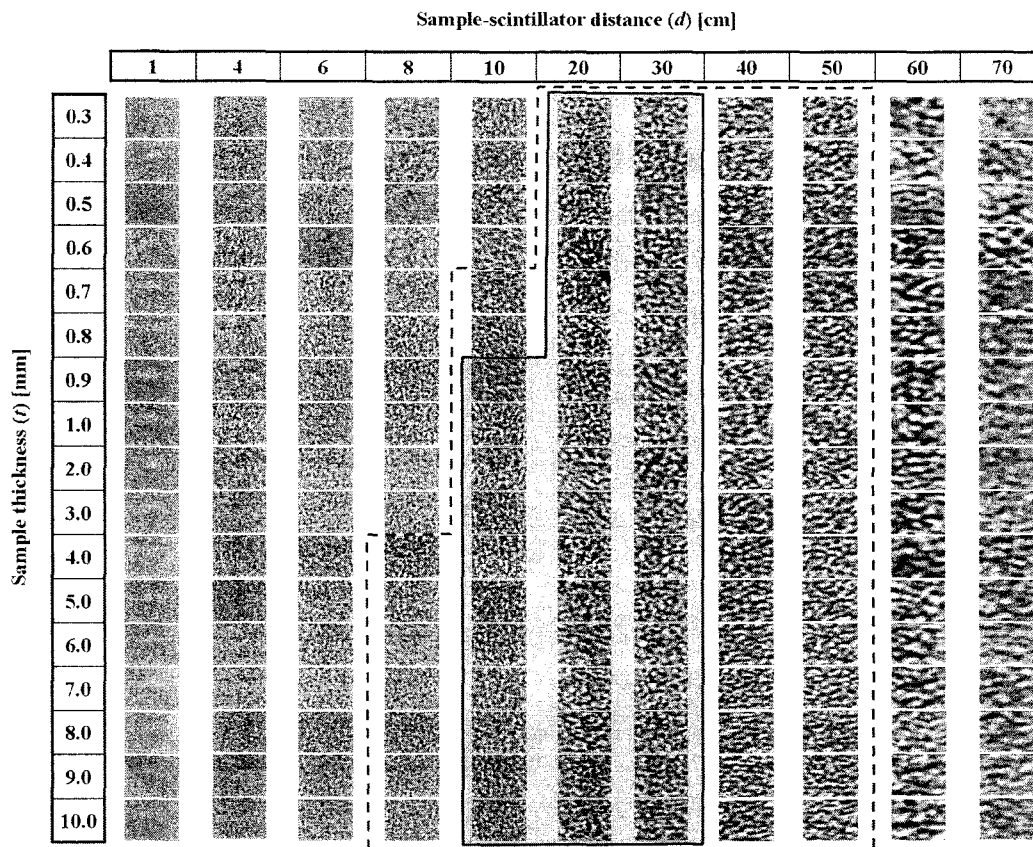


**Figure 2.** X-ray images of blood captured using the phase-contrast/interference-based enhancement method

We investigated systematically the effects of two parameters, the sample-to-scintillator distance and the sample thickness, on the speckle patterns appeared on x-ray images of tested blood samples. Figure 2 shows x-ray images of blood flow captured using the phase-contrast/ interference-based edge enhancement method. Due to the phase-contrast enhancement, the blood image becomes to show flow pattern with increasing the distance  $d$ . When  $d$  is larger than 8 cm, the speckle pattern is recognizable for all thickness tested in this study. When the distance  $d$  is over 40 cm, however, the blood patterns begin to be blurry slightly due to excessive phase-contrast enhancement. Nevertheless the blood images inside the solid-line box are still reasonably recognizable, suitable for applying PIV algorithm to extract velocity field information. In the viewpoint of interference enhancement, all patterns of blood sample with thickness  $t = 0.3\sim 10$  mm are recognizable, if the sample-to-scintillator distance  $d$  is selected properly. In particular, the x-ray images of a blood sample with 10 mm thickness show good permeability of x-ray beam, even though visualization of such a sample of large thickness using a synchrotron x-ray source would generally be difficult. From these results, we can see that this x-ray imaging technique can be applied to blood flows in large blood vessels.

To analyze the speckle patterns enhanced by the diffraction mechanism in detail, we selected four speckle pattern images from figure 2 captured at distances of  $d = 1, 10, 40,$  and  $60$  cm with fixing the sample thickness at  $1$  mm. Figure 3 shows the intensity profiles extracted from the four speckle patterns along the *vertical* direction. When the sample-to-scintillator distance is  $d = 1$  cm, the intensity profile is nearly uniform; the average gray level is about 130 and the variation is less than 20. When  $d$  is increased to  $d = 10$  cm, however, the intensity profile shows the pattern with increased clarity; the variation in the gray level in the intensity profile is about  $\pm 100$ . The

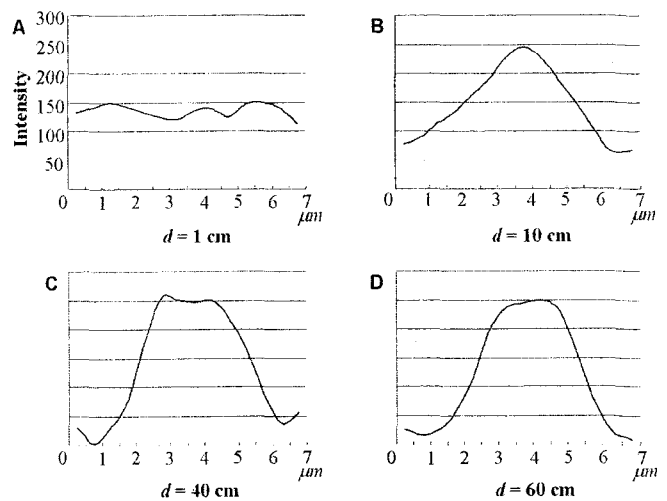


**Figure 3.** Intensity profiles along the vertical direction of speckle patterns captured

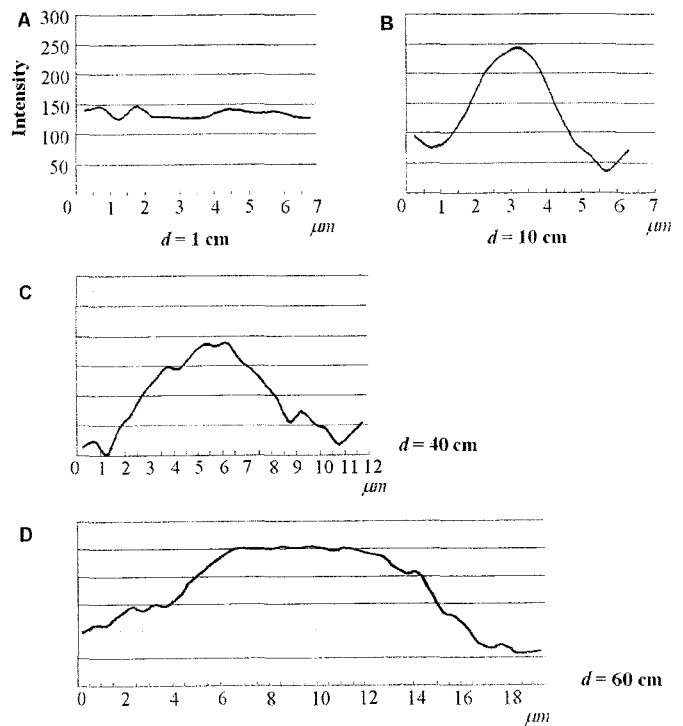


**Figure 4.** Intensity profiles along the horizontal direction of speckle patterns captured

size of the speckle pattern is about  $6\sim 7$   $\mu\text{m}$ , which is close to the size of RBCs. The size of this speckle pattern and large variation in the gray level are maintained when  $d$  is further increased to 60 cm.

Figure 4 shows intensity profiles along the *horizontal* line of the speckle patterns at sample-to-scintillator distances of  $d = 1, 10, 40$  and  $60$  cm with a

fixed sample thickness of  $t = 1$  mm. For  $d = 1$  and 10 cm, the intensity profiles resemble the corresponding profiles taken along the vertical direction (fig. 4A and 4B respectively). When  $d$  is increased further, however, the size of the speckle pattern in the horizontal direction increases continuously. This trend, which is quite different from the images observed along the vertical direction, is results from the features of the 7B2 bending magnet beam line used in this study. In a bending magnet beam, this divergence angle in the horizontal direction is usually larger than that in the vertical direction. For the 7B2 beam line, the divergence angle in the horizontal direction is about 3 mrad, whereas the angle in the vertical direction is almost zero. As a result, the diffraction-based enhancement along the horizontal direction is blurrier than that along the vertical direction. This type of non-symmetric diffraction can be improved by using an insertion device such as an undulator or wiggler.

Another optical peculiarity of blood on the synchrotron x-ray imaging method is that when an x-ray beam passes through a thick blood sample, the x-rays will pass through many layers of blood cells, causing a number of individual speckle patterns to be superimposed in the resulting x-ray image. Interestingly, in the x-ray imaging of blood, the superimposed pattern of a blood sample appearing is clearly distinguishable and has nearly uniform size, similar to the size of RBCs.

From figures 3 and 4, we can see that a sample-to-scintillator distance of  $d = 10\text{--}30$  cm gives the best speckle patterns for visualizing real blood. It should be noted that this optimum value of  $d$  will depend on the spatial resolution of the detector used, beam characteristics of the x-ray source, layout and alignment of the x-ray imaging system.

To investigate the effect of blood composition (RBCs and plasma) on x-ray imaging, we captured x-ray images of blood samples with 14 different RBC concentrations under the same conditions of  $d = 20$  cm

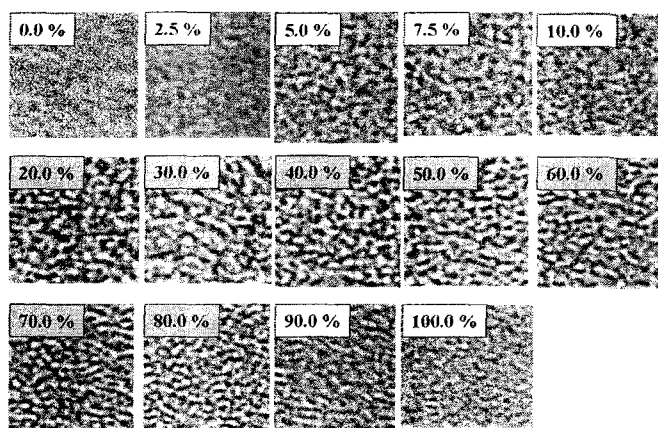


**Figure 5.** Speckle patterns of blood for different hematocrit ( $H$ )

and  $t = 2$  mm. The volume fractions of RBCs (hematocrit;  $H$ ) tested were  $H = 0.0, 2.5, 5.0, 7.5, 10.0, 20.0, 30.0, 40.0, 50.0, 60.0, 70.0, 80.0, 90.0,$  and  $100.0\%$ , where,  $H = 0\%$  corresponds to pure plasma and  $H=100\%$  to pure RBCs. In general, hematocrit for whole blood of humans is  $37\text{--}45\%$ . As can be seen in figure 5, the x-ray images of the samples with  $H = 0\text{--}10.0\%$  start to show discernable speckle patterns. In particular, distinct speckle patterns are obtained in the range of  $H = 20.0\text{--}80.0\%$ . Interestingly, the speckle pattern disappears for  $H \geq 90.0\%$ , suggesting that a certain amount of plasma, which differs from RBCs in terms of refractive index and density, is required to enhance the RBC speckle patterns. Blood with high hematocrit may therefore be visualized as having a single refractive index; hence no diffraction, interference or refraction will be induced at the edges of RBCs in such blood samples. Fortunately, however, the range of hematocrit of great interest to researchers in the fields of hemodynamics and circulatory vascular diseases is between  $H = 20.0\text{--}80.0\%$  at least.

### **X-ray PIV measurements of blood flow**

Using the phase-contrast and interference-based edge enhancement methods of synchrotron x-ray micro-imaging, it is possible to directly visualize blood flow in an opaque conduit without seeding any tracer particles

or contrast materials. The experiments were carried out at 7B2 beam line of PLS. A schematic diagram of the experimental setup for the x-ray PIV measurements is shown in Fig. 6. The x-ray images were captured with a cooled CCD camera (PCO Sencicam) with  $1280 \times 1024$  pixels resolution, after converting the x-rays to visible light using a thin  $\text{CdWO}_4$  scintillator crystal. The spatial resolution ( $\Delta y$  and  $\Delta z$ ) of the CCD camera was about  $0.67 \mu\text{m}$  and the field of view was about  $514 \times 686 \mu\text{m}^2$  in physical size, when the camera was coupled with a  $10\times$  objective lens.

Because the x-ray beam was supplied continuously, we installed a mechanical shutter to generate a pulse-type x-ray beam for PIV measurements. A delay generator was used to synchronize the mechanical shutter and the CCD camera. A syringe pump was employed to supply blood into the microchannel installed vertically. We captured x-ray images of blood flow in a rectangular-shaped opaque microchannel of  $490 \mu\text{m}$  width and  $1390 \mu\text{m}$  depth under the optimized conditions of the sample-to-scintillator distance (40 cm) and sample thickness ( $1390 \mu\text{m}$ ). By applying a two-frame cross-correlation PIV algorithm to the x-ray images of the blood flow, we could obtain instantaneous velocity fields without any artificial tracer particles. Each x-ray image was divided into many small interrogation windows of  $13 \times 13 \mu\text{m}^2$  in physical size. The speckle pattern appeared in x-ray images shows different displacement with respect to the distance from the wall. The length of displacement increases with going from the wall to the center region of the microchannel. This indicates that the displacement of speckle pattern contains information on transportation of blood cells.

The mean velocity field was obtained by ensemble averaging 200 consecutive instantaneous velocity fields statistically. The measured streamwise mean velocity field is shown in Fig. 7.<sup>4</sup> The flow speed increases with going toward the channel center from the channel wall.

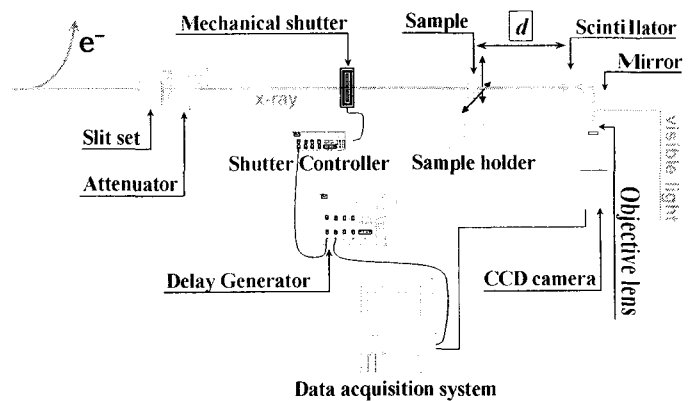


Figure 6. Schematic diagram of x-ray PIV system

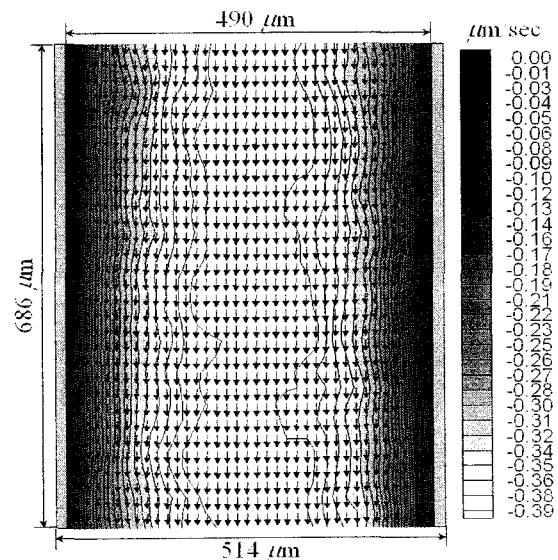


Figure 7. Streamwise mean velocity field of blood flow measured in an opaque microchannel

This velocity field is similar to the velocity distribution commonly observed in a macro-sized channel of a rectangular cross-section. This quantitative velocity field result shows the reliability of x-ray PIV method for measuring blood flows.

We also investigated blood flow inside an opaque tube with a circular cross-section. This is a realistic application of the x-ray PIV method for analyzing the non-Newtonian flow characteristics of real blood flows. Inner diameter of the opaque tube was 2.77 mm and blood was injected by a syringe pump at a flow rate of  $50 \mu\text{l}/\text{min}$ . Exposure time for acquiring each x-ray image was 20 ms.

Figure 8 shows a typical streamwise mean velocity

profile extracted from the mean velocity field data along a horizontal line. From the results of mean velocity profiles of real blood flow, we compared the experimental velocity profile with hemorheologic models of blood flow. As far as we surveyed, there is no quantitative flow information of real blood flow measured non-invasively with a high spatial resolution. It is the first trial to evaluate the hemorheologic models with the corresponding experimental results. Figure 8 shows that the measured velocity profile is well agreed with the velocity profile suggested by Casson model.<sup>14,15</sup> The typical parabolic velocity profile of Newtonian flows has some discrepancy with the experimental result. The diameter of potential core region in which no velocity gradient exists due to the yield stress of blood is  $r_c / R = 0.044$ . Conclusively, we found that the x-ray PIV method can be used for revealing various hemodynamic phenomena experimentally.

### Conclusion:

We optimized the experimental condition such as sample(blood)-to-scintillator distance, sample thickness, and hematocrit to acquire suitable x-ray images of blood flow for x-ray PIV measurements. As the sample-scintillator distance increases, the flow pattern becomes detectable with the induced phase-contrast enhancement. The optimum distance for blood sample was about 10–40 cm. The developed x-ray imaging technique was found to give suitable flow images for blood samples thicker than 1 mm. For hematocrit in the range of 20.0–80.0 %, the x-ray blood pattern is also clearly visible.

The x-ray PIV technique was applied to blood flows in an opaque rectangular microchannel. The measured velocity field data are reasonably agreed with the theoretical results. We applied the x-ray PIV method to measure blood flow in a circular tube for analyzing its non-Newtonian flow characteristics. The x-ray PIV results are well matched with the Casson's

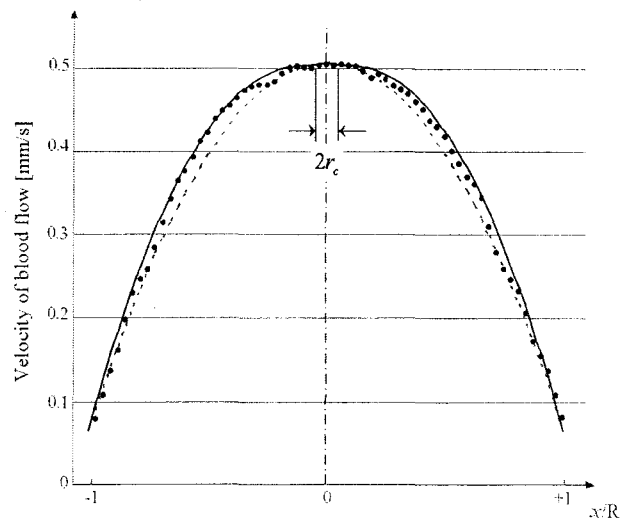


**Figure 8.** Comparison of streamwise mean velocity profile of a blood flow inside a circular tube. ●●●: X-ray PIV result; - - - : Parabolic curve fitting on the x-ray PIV result; — : Casson model fitting on the x-ray PIV result

hemorheologic model. The x-ray PIV method has a strong potential for visualizing blood flow non-invasively to obtain detailed flow information such as flow rate, spatial distributions of flow velocity and shear stress. We hope the developed x-ray PIV method can be used to investigate various hemodynamic phenomena for which the hemodynamics and pathology of circulatory diseases play a key role.

### Acknowledgement:

Experiments at the 7B2 beamline of PLS were supported in part by MOST and POSTECH. This work was also supported by MOST (KOSEF) through grant no. (R01-2004-000-10500-0) from the Basic Research Program and Systems Bio-Dynamics Research Center.

### References:

1. Park CW, Kim GB, Lee SJ. Micro-PIV measurements of blood flow in a microchannel. Presented at the International Symposium on Biomedical Optics, San Jose, USA 2004;5325-09:24-29.



2. Malek A, Alper S, Izumo S. Hemodynamic shear stress and its role in atherosclerosis. *JAMA* 1999;282:2035.
3. Lee SJ, Kim GB. X-ray particle image velocimetry for measuring quantitative flow information inside opaque objects. *J Appl Phys* 2003;94:3620.
4. Lee SJ, Kim GB. Synchrotron micro-imaging technique for measuring the velocity field of real blood flows. *J Appl Phys* 2005;97:064701.
5. Snigirev A, Snigireva I, Kohn V, Kuznetsov S, Schelokov I. On the possibilities of x-ray phase contrast microimaging by coherent high-energy synchrotron radiation. *Rev Sci Instrum* 1995;66:5486.
6. Chapman D, Thomlinson W, Johnston R E, Washburn D, Pisano E, Gmur N, Zhong Z, Menk R, Arfelli F, Sayers D. Diffraction enhanced x-ray imaging. *Phys Med Biol* 1997;42:2015.
7. Pogany A, Gao D, Wilkins S W. Contrast and resolution in imaging with a microfocus x-ray source. *Rev Sci Instrum* 1997;68:2774.
8. Nugent KA, Gureyev TE, Cookson DF, Paganin D, Barnea Z. Quantitative phase imaging using hard x rays. *Phys Rev Lett* 1996;77:2961.
9. Hu ZH, Thomas PA, Snigirev A, Snigireva I, Souvorov A, Smith PGR, Ross GW, Teat S. Phase-mapping of periodically domain-inverted LiNbO<sub>3</sub> with coherent X-rays. *Nature* 1998;392:690.
10. Spanne P, Raven C, Snigireva I, Snigirev A. In-line holography and phase-contrast microtomography with high energy x-rays. *Phys Med Biol* 1999;44:741.
11. Gureyev TE, Raven C, Snigirev A, Snigireva I, Wilkins SW. Hard x-ray quantitative non-interferometric phase-contrast microscopy. *J Phys D* 1999;32:563.
12. Kagoshima Y, Ibuki T, Yokoyama Y, Tsusaka Y, Matsui J, Takai K, Aino M. 10keV x-ray phase-contrast microscopy of observing transparent specimens. *Jpn J Appl Phys* 2001;40:L1190.
13. Je JH, Baik S, Kim HS, Jeong MH, Lee CS, Hwu Y, Margaritondo G. International consortium on phase contrast imaging and radiology beamline at the Pohang Light Source. *Rev Sci Instrum* 2004;75:4355.
14. Syoten O. *Cardiovascular Hemorheology*. Cambridge University Press 1981;40-43.
15. Macosko CW. *Rheology Principles, Measurements and Applications*. Wiley-VCH 1994;95-96.